High-Throughput Screening

Deutsche Ausgabe: DOI: 10.1002/ange.201601096
Internationale Ausgabe: DOI: 10.1002/anie.201601096

MALDI-MS Patterning of Caspase Activities and Its Application in the Assessment of Drug Resistance

*Junjie Hu[+], Fei Liu[+], and Huangxian Ju**

Abstract: *Mass spectrometry (MS) has been widely used for enzyme activity assays. Herein, we propose a MALDI-MS patterning strategy for the convenient visual presentation of multiple enzyme activities with an easy-to-prepare chip. The array-based caspase-activity patterned chip (Casp-PC) is fabricated by hydrophobically assembling different phospholipid-tagged peptide substrates on a modified ITO slide. The advantages of amphipathic phospholipids lead to high-quality mass spectra for imaging analysis. Upon the respective cleavage of these substrates by different caspases, such as caspase-1, -2, -3, and -8, to produce a mass shift, the enzyme activities can be directly evaluated by MALDI-MS patterning by m/z-dependent imaging of the cleavage products. The ability to identify drug-sensitive/resistant cancer cells and assess the curative effects of anticancer drugs is demonstrated, indicating the applicability of the method and the designed chip.*

In recent years, mass spectrometry (MS) has been proven to be a powerful method for enzyme activity assays owing to the advantages of high-throughput and label-free analyses.[1–3] However, its application is often limited by complicated sample pretreatments, including separation, purification, and desalting procedures.[4–6] To solve these problems, several gold chips with covalently assembled oligoethylene disulfide chains have been proposed for profiling the activities of kinases,[7] proteases,[8] and glycotransferases[9] and for identifying enzyme inhibitors,[10] and some aluminum oxide, gold, and ITO slides with immobilized glycan substrates have been developed for studying enzymatic reactions and protein binding.[11–13] Despite the great convenience of these on-chip MALDI-MS assays, only one oligoethylene-based chip has already been utilized for multiple enzyme assays[7] and real samples.[8] Furthermore, no patterning method to visualize multiple enzyme activities has been reported owing to the lack of methods for acquiring clear and high-quality mass spectra of complex samples.

The signal intensity is key to the development of MALDI-MS-based patterning strategies, and depends on the surface coverage, the enzyme accessibility to the chip, and the exclusion of matrix and nonspecific interference signals. Although optimal surface coverages have been achieved for enzyme activity analysis, the high hydrophobicity of the self-assembled support monolayers is unfavorable to enzyme accession.[7–9,12] Thus a hexa(ethylene glycol) spacer has been added in the bidentate linker to improve the enzyme accessibility and decrease nonspecific adsorption,[10,13] which provides the signal intensity required for the MS readout and MALDI imaging.[13] To utilize MALDI imaging for multiple enzyme assays and the related drug screening, we herein report the fabrication of a phospholipid-structured chip by noncovalent assembly of phospholipid-conjugated peptide substrates. The amphipathic phospholipids ensure the assembly of 1,2-dioctadecanoyl-*sn*-glycero-3-phosphoethanolamine (DSPE) on the hydrophobic layer conjugated to the ITO surface, and effectively enhance the biocompatibility of the surface by mimicking the composition of biological membranes,[14] which improves the enzyme accessibility, particularly in complex biosamples. Furthermore, the phospholipid tag increases the molecular weight of the enzymatic product, avoiding interference with the matrix signals, and is sensitive to MS analysis in the negative-ion mode.[15] These advantages lead to high-quality mass spectra and high MS intensity for the MALDI-MS patterning of multiple enzyme activities (Figure 1 A).

To demonstrate the utility of the patterning method for multiple enzyme assays, this strategy was used for the analysis of intracellular caspases, which usually regulate cell death.[16] Moreover, the caspase family is the main target of most chemotherapeutic agents, which usually presents different activations in drug-resistant cells.[17–22] Thus the multiple-patterning analysis of caspase activities is of great significance for monitoring the progress of an oncology therapy as well as for identifying drug resistance to adjust the treatment program.

Commercial ITO slides were chosen as the base for constructing the array-based caspase-activity patterned chips (Casp-PC). A robust and well-developed two-step modification of the slides led to a hydrophobic surface with a contact angle of 111.5° (Supporting Information, Figure S1).[13] Taking caspases-1, -2, -3, and -8 (casp) as representative target proteases,[16] their respective substrates, DSPE–PEG_2–peptide (DP1–DP4; Table S1), were prepared and embedded in different rows of the hydrophobic surface to form the Casp-PC. The chip was then used to assay multiple caspase activities by treating the array spots with the corresponding targets, which could enzymatically cleave the DPs at the C-terminal of the Asp residue, along with the loss of a dipeptide Ser–Gly–NH_2 segment to produce a mass shift. The activity patterns could thus be obtained by the *m*/*z*-dependent imaging of the products (CDPs) by a MALDI-MS

[*] J. Hu,[+] F. Liu,[+] Prof. H. Ju
State Key Laboratory of Analytical Chemistry for Life Science
School of Chemistry and Chemical Engineering
Nanjing University
Nanjing 210023 (P.R. China)
E-mail: hxju@nju.edu.cn
[+] These authors contributed equally.

Supporting information for this article can be found under: http://dx.doi.org/10.1002/anie.201601096.

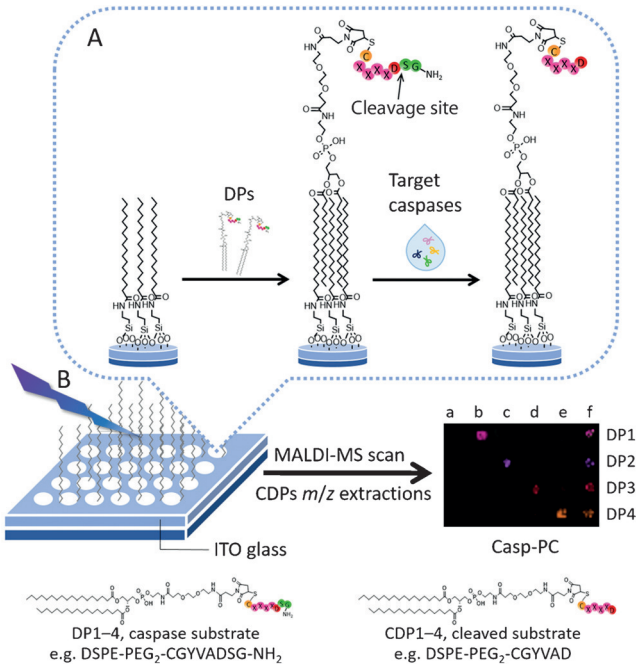

Figure 1. A) DP substrate immobilization on a stearic acid modified ITO slide through hydrophobic interactions and on-chip peptide cleavage by caspase to obtain the product CDP. B) Casp-PC patterning by a MALDI-MS scan with the *m*/*z* of CDP1–CDP4 for visual assessment of the enzyme activities.

scan (Figure 1). One DP array with 24 spots (4 rows × 6 columns) could simultaneously detect four caspases in six samples (Figure 1B), which provides a promising application for the high-throughput determination of caspase activities.

The synthesis of DSPE–PEG_2–maleimide and DP1–DP4 for the preparation of the Casp-PC (Schemes S1–S3) was confirmed by MALDI-TOF MS (Figures S2–S4). A photograph of the DHB-spotted Casp-PC showed a 4 × 6 array with acceptable spot morphology and uniform distribution (Figure 2A), which was further confirmed by the fluorescence image (Figure S5). A MALDI-MS scan of the Casp-PC produced a clear image of the extracted ions with *m*/*z* values of 1868.1, 1919.3, 1877.0, and 1935.6 for DP1–DP4, respectively (Figure 2B). The image along with *m*/*z*-dependent color coding was free of cross-contamination from adjacent spots, demonstrating the successful construction of the Casp-PC.

To test the response of the DP substrates to the target proteases, the Casp-PC spots were incubated with the corresponding caspases and their mixtures in an assay buffer. Compared with the blank, the one-to-one enzymatic reaction between DP1–DP4 and the individual casp-1, -2, -3, and -8 showed a sharp signal decrease for the extracted ion of the DP substrates and new MS signals corresponding to the cleaved peptide products at the same spots (Figure 3A, a–e). Furthermore, interference between the target proteases could be excluded. This device thus enables the simultaneous analysis of multiple caspase activities in a single sample (Figure 3A, column f). As predicted, the component that had been removed in the cleaved peptide products was demonstrated to be Ser–Gly–NH_2 (Figure S6), which led to the peptide peaks at *m*/*z* values 142.5 units lower than those shown in Figure S4. To obtain more detailed information, mass spectra could be extracted from the individual spots (Figure 3B). From the signal intensity, the cleavage efficiency of the DP substrates by the corresponding caspases could be calculated to assess the enzyme activities according to $[I_{CDP}/(I_{CDP}+I_{DP})]\times 100\,\%$, where I_{DP} and I_{CDP} are the peak intensities of the immobilized DPs and CDPs, respectively. At an optimized incubation time of 30 min (Figure S7), the

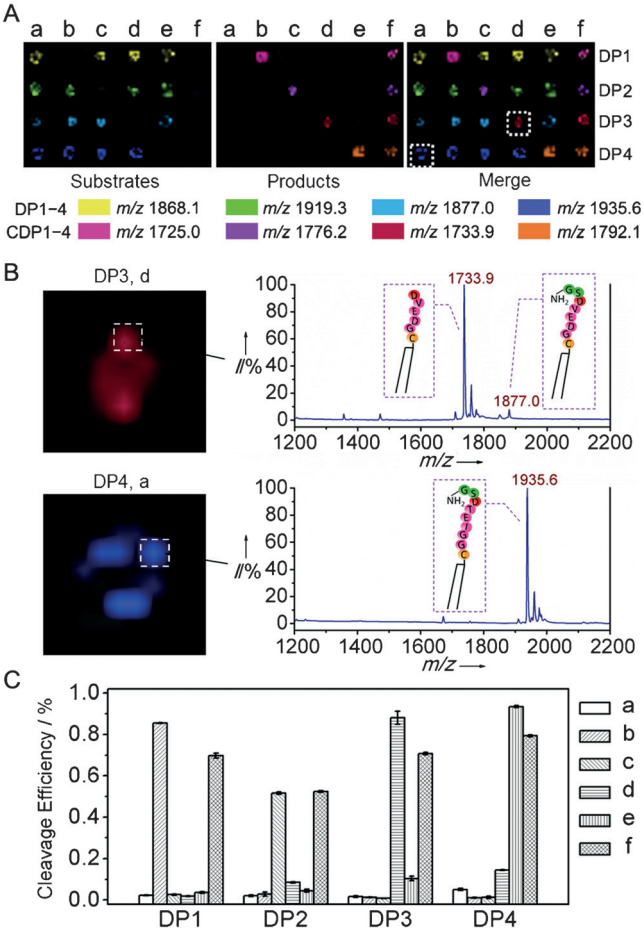

Figure 3. Enzymatic reaction specificity of caspases on Casp-PC. A) MALDI-MS images of the DP array with *m*/*z*-dependent color coding of the substrates (left) and products (middle) after treatment with a) blank, b) 50 mU casp-1, c) 20 mU casp-2, d) 60 mU casp-3, e) 100 mU casp-8, and f) an equimolar mixture of casp-1, -2, -3, and -8, and the merge of the two MALDI-MS images (right). B) Representative mass spectra extracted from individual spots. C) Cleavage efficiencies of the DPs for each spot in (A). Averages of at least three independent measurements are shown.

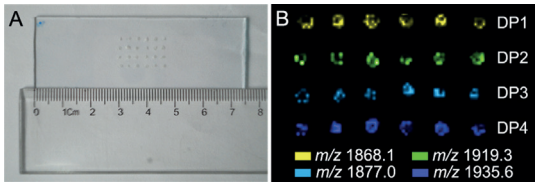

Figure 2. Characterization of Casp-PC. A) Photograph of Casp-PC with DHB spotted on each spot. B) MALDI-MS image of the DP array with *m*/*z*-dependent color coding. Representative mass spectra are shown in the Supporting Information.

caspases at the corresponding DP spots showed maximum cleavage efficiency (Figure 3C), which demonstrated the cleavage specificity of the DPs towards their target caspases.

For quantitative analysis, assay buffers (1 μL) containing various concentrations of casp-1, -2, -3, and -8 were dropped onto the corresponding spots and left to react for 30 min. Plots of the cleavage efficiency versus the logarithm of the target caspase concentration showed acceptable linearity (Figure 4A,B), which could detect the caspases at concentrations as low as 0.25, 0.1, 0.3, and 0.5 mU μL^{-1} for casp-1, -2, -3, and -8, respectively. As a control, reaction mixtures of P1–P4 and the corresponding caspases showed relatively weak signals in a MALDI chip with the same matrix, which could hardly be extracted for visualization (Figure S8), demonstrating the necessity of high-quality mass spectra for MALDI-MS imaging.

Based on the multiple enzyme assays, the Casp–PC could be used to evaluate the inhibition of caspases with different compounds. Using Ac-LETD-CHO and Ac-AAVALLPAVL-LALLAPVAD-al (casp-inh) as the inhibitors, the MALDI-MS images showed that inhibition by Ac-LETD-CHO was specific to casp-8, whereas casp-inh inhibits all four caspases (Figure 4C). The IC_{50} values of Ac-LETD-CHO and casp-inh for casp-8 were estimated to be 6.71 nM and 293.77 μM, respectively (Figure S9).

As an extended application, this strategy was used to present the caspase activities in cancer cells during chemotherapy. Human-breast-cancer MCF-7 cells were selected as a model to validate the feasibility. Doxorubicin (DOX) is a widely used antitumor drug that induces cell death by caspase activation.[23] The MCF-7 cells were seeded in 24 well plates, treated with DOX for different periods of time, harvested, and lysed by mixing the resuspended cells with glass beads. Bright-field microscopic images demonstrated that lysis was induced by vortexing the mixture for 10 min (Figure S10). After 1 μL of the supernatants of the cell lysates had been directly dropped on the different spots of the Casp-PC for enzymatic reactions, the MALDI-MS image of the left products on Casp-PC was recorded (Figure S11), which suggested that casp-1 was rarely activated, and the signals that represent casp-3 activity were also very weak. This is probably due to the loss of functional casp-3 in MCF-7 cells.[24,25] In contrast, spots related to the activities of casp-2 and casp-8 showed successively increasing brightness and reached a maximum at 24 h, which hinted at an increase in cleavage efficiency (Figure 5) and indicated the activation of the corresponding protease.[26,27]

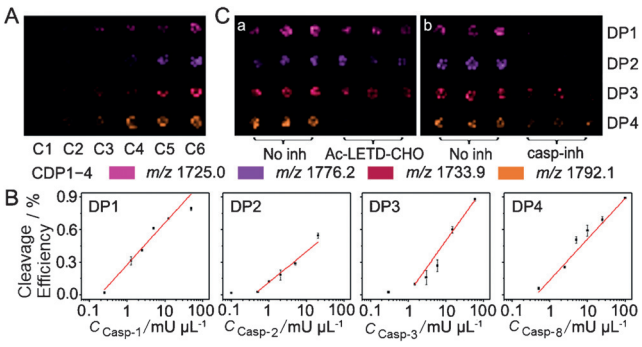

Figure 4. Quantitative analysis of the caspase activities and inhibitor screening. A) MALDI-MS image of the CDP1–CDP4 left on Casp-PC after incubation with 0, 1.25, 2.5, 5.0, 12.5, and 50 mU μL^{-1} (C1–C6) casp-1 for DP1; 0, 0.5, 1.0, 2.0, 5.0, and 20 mU μL^{-1} casp-2 for DP2; 0, 1.5, 3.0, 6.0, 15, and 60 mU μL^{-1} casp-3 for DP3; and 0, 2.5, 5.0, 10, 25, and 100 mU μL^{-1} casp-8 for DP4. B) The cleavage efficiency of DP1–DP4 as a function of the logarithm of the casp-1, -2, -3, and -8 concentrations. C) MALDI-MS images after incubation with caspase mixtures in the absence (first three columns) and presence (last three columns) of inhibitors.

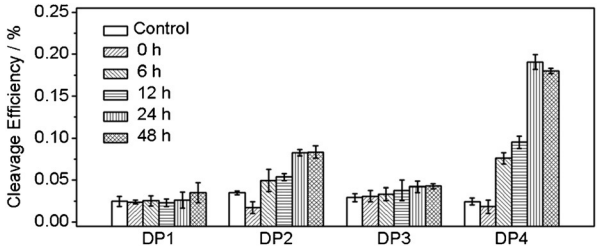

Figure 5. Treatment-time-dependent activation of casp-1, -2, -3, and -8 in lysates of MCF-7 cells treated with 1.0 μg mL^{-1} DOX determined with the Casp-PC after incubation for 30 min.

For comparison, DOX-resistant MCF/ADR cells and MCF-7 cells were treated with 0–10 μg mL^{-1} DOX for 24 h. With an increased amount of DOX, they did not show casp-1 activation, whereas the DP2 and DP4 spots, corresponding to casp-2 and -8, gradually increased in intensity on both chips (Figure S12), suggesting different dose dependences for the intracellular activation of different caspases. However, the MCF-7 cells were much more sensitive to DOX than the MCF/ADR cells, and the corresponding caspases were found to be activated at a rather low concentration of DOX (Figure 6A). A similar intensity could be observed for MCF/ADR cells at a 50 times higher DOX concentration. This may arise from the overexpression of the plasma-membrane P-glycoprotein (Pgp) transporters in MCF/ADR cells, which increases the drug efflux and thus prevents the activation of caspase-induced programmed cell death.[28,29] Furthermore, unlike for the MCF-7 cells, casp-3 activity was detected in MCF/ADR cells, which is consistent with a previous report.[30] Flow-cytometric assays of the same treated cells using the Annexin V-APC/7-AAD apoptotic kit also validated the caspase-dependent cell apoptosis (Figure 6B). The apoptosis rates for MCF-7 cells treated with 1.0 and 10 μg mL^{-1} DOX were 71.5% and 91.4%, respectively, whereas MCF/ADR cells did not show significant apoptosis when exposed to 1.0 μg mL^{-1} DOX, and only 11.4% of the cells underwent apoptosis at 10 μg mL^{-1} DOX. These results are in good agreement with those from the caspase activity patterns, demonstrating the feasibility of the Casp-PC and the proposed MALDI-MS patterning strategy as a promising method for the assessment of drug resistance and the discrimination of drug-sensitive/resistant cancer cells.

In conclusion, using a newly synthesized amphipathic phospholipid as the tagged ligand, an array-based caspase-activity patterned chip with good enzyme accessibility has been conveniently prepared, and a MALDI-MS patterning

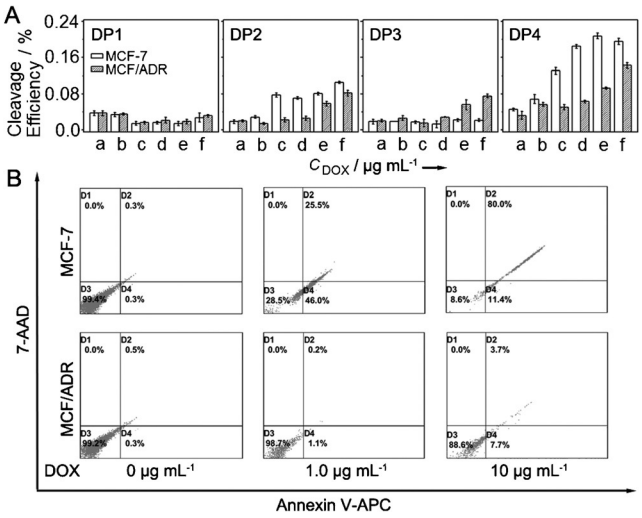

Figure 6. Caspase activities in DOX-treated MCF-7 and MCF/ADR cells. A) Cleavage efficiency of the DPs on Casp-PC after 30 min incubation with lysates of MCF-7 and MCF/ADR cells treated with a) 0, b) 0.1, c) 0.5, d) 1.0, e) 5.0, and f) 10.0 μg mL^{-1} DOX for 24 h. B) Flow-cytometric analysis of cells treated as in (A) with the dual fluorescence of Annexin V-APC/7-AAD.

strategy for the label-free analysis of multiple enzyme activities has been developed. The amphipathic ligand assures the assembly of the hydrophobic components and the biocompatibility for enzyme access, which leads to high-sensitivity and high-quality mass spectra for MALDI-MS imaging analysis. Through the *m*/*z*-dependent coding, this MS-based imaging platform possesses great flexibility in designing peptide substrates to achieve high selectivity for individual caspases, and makes it possible to visualize the caspase activities of different cells. It is suitable for the identification of drug resistance and the high-throughput screening of anticancer agents. This work provides a new opportunity to explore the enzyme activity patterns in complicated physiological processes.

Acknowledgements

This research was supported by the National Natural Science Foundation of China (21135002, 21361162002), the Priority Development Areas of The National Research Foundation for the Doctoral Program of Higher Education of China (20130091130005), and a Graduate Innovation Project of Jiangsu Province (KYZZ15_0031). We thank Yubing Wang (R&D Department, Luye Pharma Co., Ltd.) for his assistance with the syntheses described in this work.

Keywords: caspases · enzymes · high-throughput screening · MALDI-MS · mass spectrometry

How to cite: *Angew. Chem. Int. Ed.* **2016**, *55*, 6667–6670
Angew. Chem. **2016**, *128*, 6779–6782

[1] A. Liesener, U. Karst, *Anal. Biochem. Chem.* **2005**, *382*, 1451–1464.
[2] S. M. Patrie, M. J. Roth, D. A. Plymire, E. Maresh, J. M. Zhang, *Anal. Chem.* **2013**, *85*, 10597–10604.
[3] J. J. Hu, F. Liu, H. X. Ju, *Anal. Chem.* **2015**, *87*, 4409–4414.
[4] X. Gu, C. H. Deng, G. Q. Yan, X. M. Zhang, *J. Proteome Res.* **2006**, *5*, 3186–3196.
[5] A. J. Percy, C. E. Parker, C. H. Borchers, *Bioanalysis* **2013**, *5*, 2837–2856.
[6] J. M. Joo, B. R. Lee, T. H. Lee, K. H. Liu, *Rapid Commun. Mass Spectrom.* **2014**, *28*, 2405–2414.
[7] D. H. Min, J. Su, M. Mrksich, *Angew. Chem. Int. Ed.* **2004**, *43*, 5973–5977; *Angew. Chem.* **2004**, *116*, 6099–6103.
[8] J. Su, T. W. Rajapaksha, M. E. Peter, M. Mrksich, *Anal. Chem.* **2006**, *78*, 4945–4951.
[9] L. Ban, N. Pettit, L. Li, A. D. Stuparu, L. Cai, W. L. Chen, W. Y. Guan, W. Q. Han, P. G. Wang, M. Mrksich, *Nat. Chem. Biol.* **2012**, *8*, 769–773.
[10] D. H. Min, W. J. Tang, M. Mrksich, *Nat. Biotechnol.* **2004**, *22*, 717–723.
[11] S. H. Chang, J. L. Han, S. Y. Tseng, H. Y. Lee, C. W. Lin, Y. C. Lin, W. Y. Jeng, A. H. J. Wang, C. Y. Wu, C. H. Wong, *J. Am. Chem. Soc.* **2010**, *132*, 13371–13380.
[12] A. Sanchez-Ruiz, S. Serna, N. Ruiz, M. Martin-Lomas, N. C. Reichardt, *Angew. Chem. Int. Ed.* **2011**, *50*, 1801–1804; *Angew. Chem.* **2011**, *123*, 1841–1844.
[13] A. Beloqui, J. Calvo, S. Serna, S. Yan, I. B. H. Wilson, M. Martin-Lomas, N. C. Reichardt, *Angew. Chem. Int. Ed.* **2013**, *52*, 7477–7481; *Angew. Chem.* **2013**, *125*, 7625–7629.
[14] L. L. Li, R. B. Zhang, L. L. Yin, K. Z. Zheng, W. P. Qin, P. R. Selvin, Y. Lu, *Angew. Chem. Int. Ed.* **2012**, *51*, 6121–6125; *Angew. Chem.* **2012**, *124*, 6225–6229.
[15] A. C. Niehoff, H. Kettling, A. Pirkl, Y. N. Chiang, K. Dreisewerd, J. Y. Yew, *Anal. Chem.* **2014**, *86*, 11086–11092.
[16] S. Shalini, L. Dorstyn, S. Dawar, S. Kumar, *Cell Death Differ.* **2015**, *22*, 526–539.
[17] S. W. Lowe, A. W. Lin, *Carcinogenesis* **2000**, *21*, 485–495.
[18] D. E. Fisher, *Cell* **1994**, *78*, 539–542.
[19] C. B. Thompson, *Science* **1995**, *267*, 1456–1462.
[20] R. C. Taylor, S. P. Cullen, S. J. Martin, *Nat. Rev. Mol. Cell Biol.* **2008**, *9*, 231–241.
[21] C. Holohan, S. V. Schaeybroeck, D. B. Longley, P. G. Johnston, *Nat. Rev. Cancer* **2013**, *13*, 714–726.
[22] X. H. Yang, T. L. Sladek, X. S. Liu, B. R. Butler, C. J. Froelich, A. D. Thor, *Cancer Res.* **2001**, *61*, 348–354.
[23] W. Cao, S. L. Ma, J. J. Tang, J. Q. Shi, Y. J. Lu, *Biochim. Biophys. Acta Mol. Cell Res.* **2006**, *1763*, 182–187.
[24] R. U. Jänicke, *Breast Cancer Res. Treat.* **2009**, *117*, 219–221.
[25] R. U. Jänicke, I. H. Engels, T. Dunkern, B. Kaina, K. Schulze-Osthoff, A. G. Porter, *Oncogene* **2001**, *20*, 5043–5053.
[26] M. Jelínek, K. Balušíková, D. Kopperová, V. Němcová-Fürstová, J. Šrámek, J. Fidlerová, I. Zanardi, I. Ojima, J. Kovár, *Cancer Cell Int.* **2013**, *13*, 42.
[27] W. H. Liu, L. S. Chang, *Int. J. Biochem. Cell Biol.* **2011**, *43*, 1708–1719.
[28] M. F. Chung, H. Y. Liu, K. J. Lin, W. T. Chia, H. W. Sung, *Angew. Chem. Int. Ed.* **2015**, *54*, 9890–9893; *Angew. Chem.* **2015**, *127*, 10028–10031.
[29] H. Meng, W. X. Mai, H. Y. Zhang, M. Xue, T. Xia, S. J. Lin, X. Wang, Y. Zhao, Z. X. Ji, J. I. Zink, A. E. Nel, *ACS Nano* **2013**, *7*, 994–1005.
[30] J. S. K. Chen, M. Konopleva, M. Andreeff, A. S. Multani, S. Pathak, K. Menta, *J. Cell. Physiol.* **2004**, *200*, 223–234.

Received: January 30, 2016
Revised: March 14, 2016
Published online: April 21, 2016

